Circulation: Genomic and Precision Medicine

ORIGINAL ARTICLE

Cardiac α-Actin (*ACTC1*) Gene Mutation Causes Atrial-Septal Defects Associated With Late-Onset Dilated Cardiomyopathy

BACKGROUND: Familial atrial septal defect (ASD) has previously been attributed primarily to mutations in cardiac transcription factors. Here, we report a large, multi-generational family (78 members) with ASD combined with a late-onset dilated cardiomyopathy and further characterize the consequences of mutant α-actin.

METHODS: We combined a genome-wide linkage analysis with cell biology, microscopy, and molecular biology tools to characterize a novel *ACTC1* (cardiac α-actin) mutation identified in association with ASD and late-onset dilated cardiomyopathy in a large, multi-generational family.

RESULTS: Using a genome-wide linkage analysis, the ASD disease locus was mapped to chromosome 15q14 harboring the *ACTC1* gene. In 15 affected family members, a heterozygous, nonsynonymous, and fully penetrant mutation (p. Gly247Asp) was identified in exon 5 of *ACTC1* that was absent in all healthy family members (n=63). In silico tools predicted deleterious consequences of this variant that was found absent in control databases. Ultrastructural analysis of myocardial tissue of one of the mutation carriers showed sarcomeric disarray, myofibrillar degeneration, and increased apoptosis, while cardiac proteomics revealed a significant increase in extracellular matrix proteins. Consistently, structural defects and increased apoptosis were also observed in neonatal rat ventricular cardiomyocytes overexpressing the mutant, but not native human ACTC1. Molecular dynamics studies and additional mechanistic analyses in cardiomyocytes confirmed actin polymerization/turnover defects, thereby affecting contractility.

CONCLUSIONS: A combined phenotype of ASD and late-onset heart failure was caused by a heterozygous, nonsynonymous ACTC1 mutation. Mechanistically, we found a shared molecular mechanism of defective actin signaling and polymerization in both cardiac development and contractile function. Detection of ACTC1 mutations in patients with ASD may thus have further clinical implications with regard to monitoring for (late-onset) dilated cardiomyopathy.

Derk Frank, MD*
Ashraf Yusuf Rangrez, PhD*
Corinna Friedrich, PhD*
Sven Dittmann, PhD*
Birgit Stallmeyer, PhD
Pankaj Yadav, PhD
Alexander Bernt, PhD
Ellen Schulze-Bahr
Ankush Borlepawar, MS
Wolfram-Hubertus Zimmermann, MD
Stefan Peischard, PhD
Guiscard Seebohm, PhD
Wolfgang A. Linke, PhD
Hideo A. Baba, MD
Marcus Krüger, PhD
Andreas Unger, PhD
Philip Usinger, MD
Norbert Frey, MD†
Eric Schulze-Bahr, MD†

*Drs Frank, Yusuf Rangrez, Friedrich, and Dittmann contributed equally to this work.

†Drs Frey, and Eric Schulze-Bahr contributed equally to this work.

Key Words: chromosomes ■ dilated cardiomyopathy ■ heart failure ■ molecular dynamics simulation ■ sarcomeres

https://www.ahajournals.org/journal/circgen

Atrial septal defect (ASD) is the third most common congenital heart disease (CHD) with an estimated incidence of 100 per 100 000 live births.[1] In the adult population of patients with CHD, ≈25% have an ASD, which suggests that 0.4% of the entire adult population has an ASD compared with a patent foramen ovale which is prevalent in about 25% of adults.[2] ASD is commonly related to mutations in cardiac transcription factors involved in atrial septal formation (eg, *NKX2-5*, *GATA4*, and *TBX5*,[3] *TBX20,*[4] or *NOTCH1*[5]). Most ASDs are sporadic without an identifiable cause and typically without autosomal dominant inheritance.[1] In addition, ASDs, in particular of the secundum type (ASD-II), are often seen nonisolated, that is, in genetic syndromes (such as Holt-Oram, Noonan, or Down syndrome). Here, we report on a very large multi-generation family with isolated ASD-II, and quite uncommonly, followed by late-onset heart failure in the setting of a dilated cardiomyopathy (DCM). After genome-wide linkage of the disease locus to microsatellite markers on chromosome 15q14, a nonsynonymous mutation in the *ACTC1* gene (p. Gly247Asp or: G247D) was identified as the cause for this combined, novel phenotype. Of note, a few heterozygous *ACTC1* gene mutations have earlier been described in isolated ASD-II[6], recessive *ACTC1* mutations are unknown so far.

The *ACTC1* gene encodes cardiac α-actin that together with regulatory proteins tropomyosin and 3 troponins (C, I, and T) forms the thin contractile filament, in turn connecting the myocellular Z-disc with the thick filament protein myosin. Actin is essential for a wide range of cell functions. Mice lacking *actc1* show embryonic or perinatal lethality and myofibrillar disarray.[7] In nonsyndromic, human DCM, *ACTC1* was the first causative gene described for autosomal dominant heart failure,[8] but to date, only a few mutations (mainly in subdomain 3) have been published (Table I in the Data Supplement). The majority of *ACTC1* mutations though have not been investigated for their functional consequence.

Given the importance of ACTC1 in the structural and functional integrity of cardiomyocytes, extending knowledge on mutant dysfunction as a cause of ASD, heart failure or CHD, per se, is of general interest and potentially of clinical importance. Through molecular and functional analysis, we found that G247D mutation causes loss of function phenotype that was characterized by a disturbed actin polymerization, increased apoptosis and sarcomeric disarray in both human samples and neonatal rat ventricular cardiomyocytes (NRVCMs), thereby causing detrimental effects on contractile function.

MATERIALS AND METHODS

The authors declare that all supporting data are available either within the article (in the Data Supplement) or will be available on a request to the corresponding author. Detailed information on the genotyping and variant classification, cardiac pathology and protein identification, characterization of mutant ACTC1 protein in rat cardiomyocytes and assays for viability, reporter gene and Rho G-LISA and molecular dynamics simulation as well as contractility measurements are provided in the Data Supplement.

The study was approved by an institutional review committee of the University of Münster (2012-174-f-N), and that the subjects gave informed consent. Details of the genetic analysis and whole/targeted genome sequencing are provided in the Data Supplement.

RESULTS

An *ACTC1* (Cardiac α-Actin) Gene Mutation Causes Autosomal Dominant Atrial Septum Defect and Late-Onset DCM In 2 Families

A large multi-generation family (>100 living family members; family identity number: 9999, Figure 1A) with an autosomal dominant inherited form of an ASD (secundum type: ASD-II) was recognized in the Northwestern parts of Germany. So far, out of 81 recruited family members with clinical evaluations, 78 members (15 affected, 63 unaffected) were available for genotyping (Figure 1A). All patients were retrospectively interrogated for cardiac surgery or interventions, signs of heart failure, arrhythmias, syncope or sudden cardiac death of relatives. In addition, a second, but small family (family identity number: 10179) with ASD and late-onset biventricular heart failure (only 2 of the affected family members were available for genotyping) originating from the same geographic area was also investigated. Clinical details of both families are listed in Table 1.

We first investigated DNA of both probands for mutations in other ASD genes (eg, *NKX2-5, GATA4, GATA6,* and *MYH6*) without identification of any causative mutation. Due to the large size of the ASD-II family, a genome-wide linkage study with 300 polymorphic microsatellite markers was performed that revealed significant linkage of the disease locus with a haplotype of markers between D15S231 (26.48 cM) and D15S118 (34.10 cM) on chromosome 15q13.3-15q14. Further haplotyping (D15S1007, 28.86 cM; D15S1040, 29.95 cM; D15S971, 32.71 cM) narrowed this region to a candidate region between D15S1040 and D15S971 (chr15:33310773-35085308) in which all affected family members shared the same marker haplotype. Further haplotyping (D15S1007, 28.86 cM; D15S1040, 29.95 cM; D15S971, 32.71 cM) narrowed this region to a candidate region (initially: 101 genes, 5.4 cM) between markers D15S1040 and D15S971 (chr15:33310773-35085308) in which again all affected family members shared the same marker haplotype. Of note, the identical haplotype was identified in the second smaller family (family identity number: 10179) with ASD and

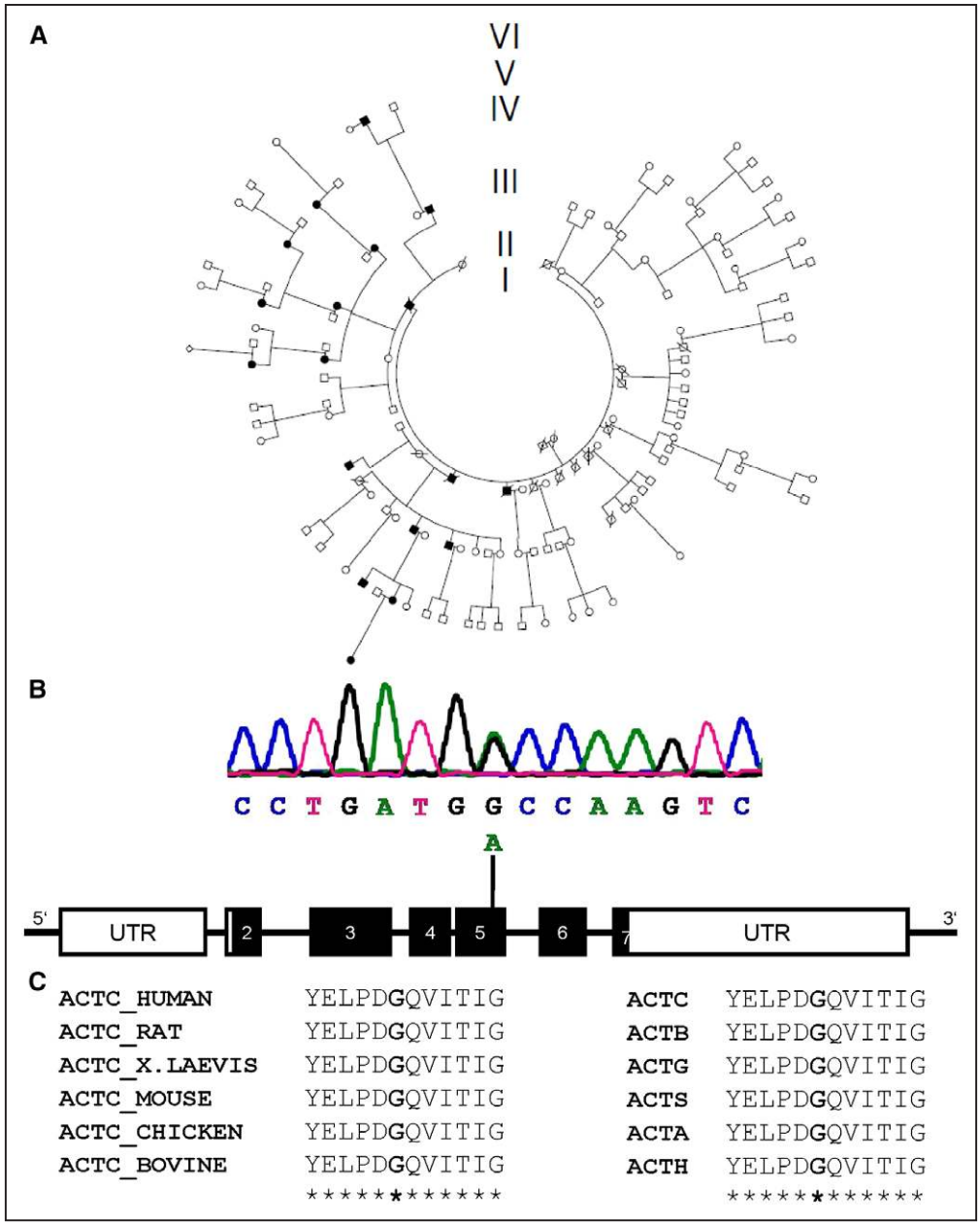

Figure 1. Genome-wide linkage study in a large multi-generation family identified a nonsynonymous ACTC1 gene mutation (c. 740 G>A; p. Gly247Asp or G247D) as causative for autosomal dominant atrial septal defect (ASD) and late-onset heart failure.
A, Pedigrees of the German family. Men are denoted by squares and women by circles. Solid symbols indicate clinically affected individuals and crossed symbols denote deceased patients. **B**, In exon 5 of *ACTC1* (chr. 15q14), a heterozygous single nucleotide exchange was identified in exon 5 (c.740G>A) only in affected family members and in another German family with the identical phenotype (not shown). **C**, Orthologous (**left**) and paralogous (**right**) alignments around the mutant ACTC1 residue. The glycine at residue 247 (bold) is highly conserved and invariant between species (**C**, **left**), but also among all related human actins (**C**, **right**).

late-onset biventricular heart failure. The candidate region contains nearly 1.8 Mb of sequence and 22 genes according to the NCBI Map Viewer (https://www.ncbi.nlm.nih.gov/projects/mapview; Table II in the Data Supplement). Apart from this locus with the 2-point lod score of 7.99 (?=0, not shown), no other chromosomal loci showed significant linkage (ie, lod score >3.0, *P* value ≤0.001) with the disease phenotype. To identify the disease-causing mutation, whole-exome sequencing on proband (9999_536) was performed. A total of 45 378 exonic or splice region variants were called (41 109 SNPs and 4269 INDELs), and 47 variants were located under the linkage peak region on chromosome 15. Next, we focused on novel or relatively rare (MAF in ExAC <0.1%) variants predicted to alter the amino acid sequence and identified a heterozygous single nucleotide variant in the cardiac α-actin gene *ACTC1* (NM_005159.4: c. 740G>A, exon 5) leading to a predicted amino acid substitution (p. Gly247Asp; Figure 1B) as the only remaining variant. This nucleotide exchange was confirmed by Sanger sequencing of two independent polymerase chain reaction products.

Table. Clinical Profile of Heterozygous *ACTC1* Mutation Carriers for p. Gly247Asp

ID	Age	ASD	ASD Closure, age	Heart Failure NYHA Class	Heart Transplantation, age	Cardiomyopathy	Other Disease
9999-0	9	Yes	3 y	I			
9999-545	49	Yes	17 y	II		DCM, LVNC	
9999-548	29	Yes	7 y	I			
9999-526	66	Yes	34 y	IV	49 y	DCM	
9999-536	58	Yes	27 y	II-III		DCM	SND, AFLA, ATFB
9999-524	31	Yes	4 y	II			Dextrocardia
9999-559	33	Yes	4 y	I			
9999-537	47	Yes	33 y	II			ATFB, AFLA
9999-557	63	Yes	27 y	IV	(none; died at 63 y)	DCM	ATFB
9999-555	48	Yes	6 y	I			
9999-539	70	Yes	Unknown	IV	55 y	DCM	
9999-580	63	No		III		DCM	ATFB
9999-583	80	Yes	Unknown	II			
9999-551	68	Yes (PFO)	36 y	I			
9999-550	51	Yes (PFO)	No	I			AVB-I°
10179-1	79	Yes	53 y	III		DCM (LV+RV)	Two brothers with closed ASD
10179-3	54	Affected by hear saying	Unknown	unknown			

AFLA indicates atrial flutter; ASD, atrial septal defect; ATFB, atrial fibrillation; AVB, atrioventricular blockade; DCM, dilated cardiomyopathy; ID, identifier; LV, left ventricle; LVNC, left ventricular noncompaction; NYHA, New York Heart Association functional classification; PFO, patent foramen ovale; RV, right ventricle; and SND, sinus node dysfunction.

In large control databases (gnomAD) and in the Human Gene Mutation Database, this single nucleotide variant was absent. The glycine residue 247 in human ACTC1 is highly conserved between species (including Baker's yeast) and present in all 6 human actin paralogues (Figure 1C). The smallest amino acid residue glycine was substituted by the larger aspartic acid and also introduced a negative charge into ACTC1. In VarCards, 20 out of 22 in silico algorithms predicted this variant to be deleterious (damaging score: 0.91)

The mutation was present in 15 affected (absent in 23 unaffected) members of the large and in 2 members of the second smaller family. The clinical phenotype was consistent with a congenital ASD-II (present in 14 mutation carriers; not in 2 with patent foramen ovale and in one with a normal septum) and progressive heart failure in the setting of DCM; the latter started typically in the fourth to fifth decade (7 mutation carriers were affected) and resulted in sudden cardiac death in one female (at the age of 63 years) and 2 heart transplantations (males, at the age of 51 and 55 years). Four of the mutation carriers developed atrial arrhythmias (flutter and fibrillation) at younger age, after ASD closure (Table 1).

We additionally performed targeted exome sequencing encompassing 49 cardiomyopathy genes on 3 other affected family members (9999_545, 9999_526, and 10179_1). In all family members, the known presence of the identified *ACTC1* mutation was confirmed, and no other cardiomyopathy mutation was detected excluding the possibility of other mutation causing the observed disease phenotype. Taken together, carriers of the p. Gly247Asp *ACTC1* mutation predominantly exhibit a congenital ASD-II (88%) with a subset developing DCM with progressive heart failure at middle age.

Immunostaining of Cardiac Tissue and Ultrastructural Analysis From an *ACTC1* Mutation Carrier (p. G247D) Shows Increased Apoptosis and Myofibrillar Disarray

We obtained a cardiac sample of an explanted heart (due to terminal heart failure) from an affected *ACTC1* mutation carrier family member at the age of 49 years. Immunostaining results for cardiac α-actinin and terminal deoxynucleotidyl transferase dUTP nick end labeling (TUNEL) assays were compared with a sample form of a healthy, nontransplanted donor heart, and from an explanted DCM heart during terminal heart failure (47 years, male). In presence of the *ACTC1* mutation, the Z-bands (visible through staining of α-actinin) showed a structural disarray in contrast to the unaffected cardiac control tissue sample and to the DCM sample (Figure 2A).

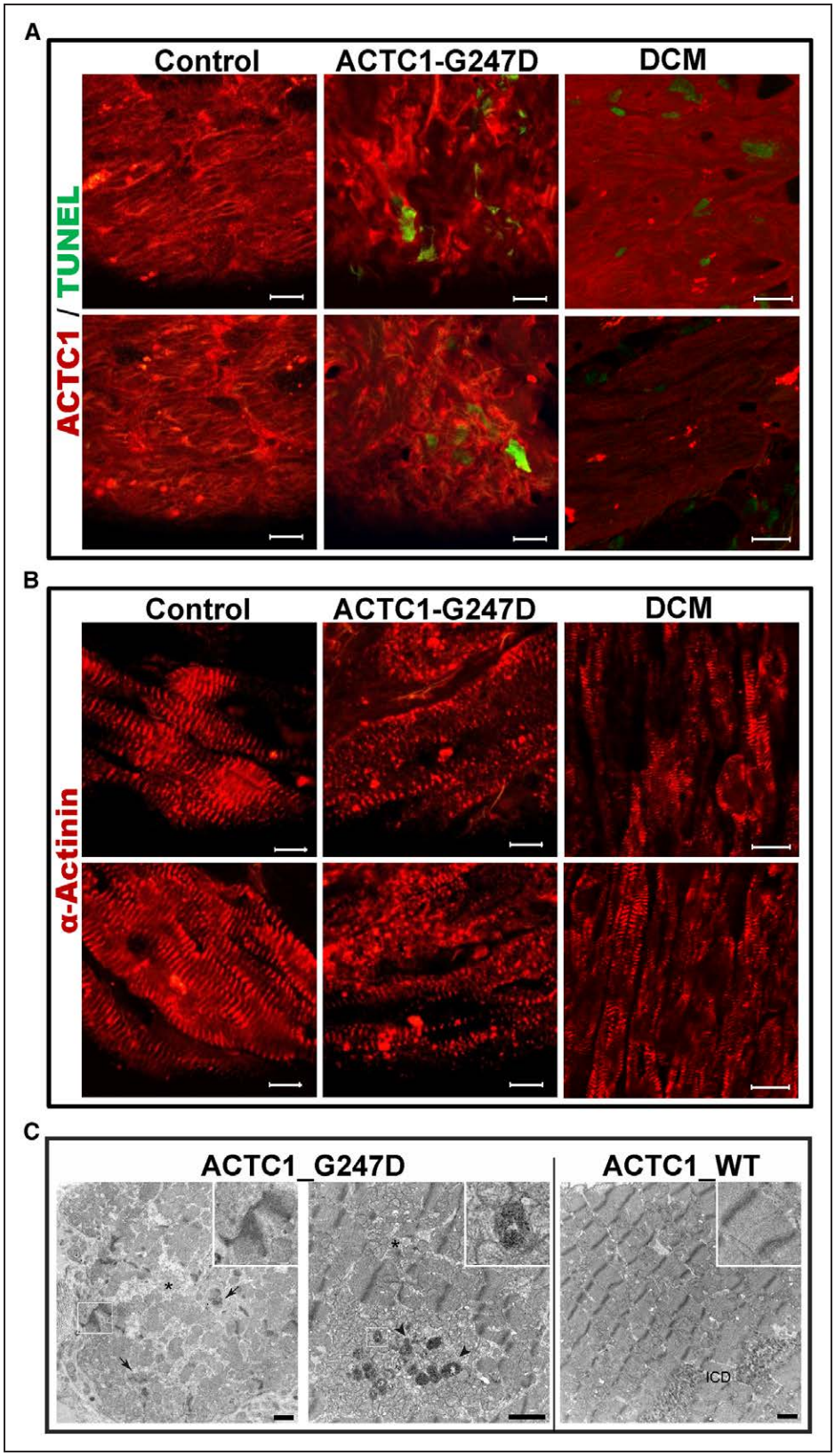

Figure 2. Characterization of cardiac tissue from an ACTC1 mutation carrier.
A, Immunohistochemistry was performed in cardiac tissue sections from a healthy control (nontransplant heart), from an ACTC1-G247D mutation carrier (explanted heart), and from a dilated cardiomyopathy (DCM) donor (explanted heart). Images show α-actinin antibody-staining in red. Stained Z-bands show an ordered structure in cardiac tissue from a healthy control (**left**, nontransplanted heart) and from a DCM tissue (**right**), whereas structure in tissue of an ACTC1-G247D mutation carrier (**middle**) was disarrayed. Magnification: for control and G247D 630× (scale bar: 10 μm), for DCM 250× (scale bar: 20 μm). (*Continued*)

Figure 2 Continued. B, Images show ACTC1 antibody-staining in red and apoptotic cells in green. Red staining was induced by a specific antibody, green-labeling of apoptotic cells was performed by the use of fluorescein-dUTP for detection of DNA-strand breaks via TUNEL-reaction. Magnification: 630×, Scale bar: 10 μm. **C**, Ultrastructural analysis of the explant of mutant ACTC1 (ACTC1_G247D) patient heart. Typical structural anomalies in the patient muscles showing wavy and streaming Z-discs (arrows, inset), autophagic vacuoles and the progressive stages of myofibrillar degeneration (asterisks) including disassembled Z-discs, loss of myofibril orientation, and enlarged, accumulated mitochondria (arrowheads, inset). Complete dissolution of the Z-disc structure and sarcomeric deterioration are culminating in complete myofibril degeneration. Control cardiac sample showed normal myofibrillar organization. Scale bar: 2 μm. ICD indicates intercalated disc; TUNEL, terminal deoxynucleotidyl transferase dUTP nick end labeling; and WT, wild-type.

In addition, a TUNEL assay for the identification of apoptotic areas showed an increased number of apoptotic cells in cardiac tissue of the *ACTC1* mutation carrier, but not in control tissue (Figure 2B). Of note, also in the cardiac tissue from the DCM heart apoptosis could also be detected but with a lower degree than in the ACTC1 mutant tissue.

We next performed ultrastructural analysis of cardiac tissue from the nontransplanted and from the mutant ACTC1 hearts using electron microscopy. Consistent with the immunofluorescence data, we observed typical structural anomalies in the patient cardiac muscles showing sarcomeric degeneration with wavy and streaming Z-discs (arrows, inset), autophagic vacuoles, and the progressive stages of myofibrillar degeneration (asterisks) including disassembled Z-discs, loss of myofibrillar orientation, and enlarged, accumulated mitochondria (arrowheads, inset; Figure 2C). Furthermore, complete dissolution of the Z-disc structure and sarcomeric deterioration culminated in complete myofibril degeneration compared with the control human heart sample (Figure 2C).

Additionally, we performed mass spectrometry with ultrasensitive protein detection and quantitation using label-free tagging to compare the protein profiles of the *ACTC1* mutation carrier and the 2 control samples. In total, 2617 proteins were identified at a false-discovery rate of <1% at the peptide and protein levels. Proteins that were not detectable in both, controls or the patient sample, were excluded from further analysis; a total of 1140 proteins remained for comparison (44% of all proteins). Notably, we identified a peptide representing the mutant ACTC1 by mass spectrometric analysis (Figure IA in the Data Supplement), but there was no difference in ACTC1 protein levels between the patient and 2 control samples. A scatter plot based on label-free protein intensities showed the varying protein intensities between the controls and mutant ACTC1 cardiac sample but not between the 2 control samples that appeared quite homogeneous (Figure IB and IC in the Data Supplement). Using a cutoff fold-change >2, we found 238 upregulated proteins (eg, several collagens, fibulin, tenascin, and elastin), whereas, 199 proteins were downregulated (eg, mitochondrial respiratory chain complex I, enzymes of the TCA cycle and fatty acid pathway, Table III). This clearly indicated severe remodeling of the extracellular matrix, fibrosis, and a reduced energy production in the ACTC1 mutant sample. Of note, we also found several sarcomeric proteins (eg, myosin light chain 7, MYL4, cysteine and glycine-rich protein 1, and Filamin A) with an enhanced protein detection (and thus potentially compensatory function) in the ACTC1 mutant sample.

Mutant ACTC1 Protein Causes Increased Apoptosis and Myofibrillar Disarray in NRVCMs

We generated adenovirus constructs for overexpression of the native (wild-type; ACTC1_WT) and mutant (ACTC1_G247D) human ACTC1 protein in NRVCMs (Figure IIA and IIB in the Data Supplement) to study cellular and functional effects in vitro. When overexpressed, ACTC1_G247D in NRVCMs showed a severe change in cell morphology, size, and sarcomeric structure (Figure 3A) when compared with the control cells (LacZ) or cells overexpressing ACTC1_WT. The cell surface area was significantly reduced in ACTC1_G247D overexpressing cells (341±136 μm^2; n>1000) when compared with nonoverexpressing cells (LacZ; 489±206 μm^2; n>1000) or cell overexpressing native ACTC1 (ACTC1_WT; [440±195 μm^2; n>1000; P<0.001; Figure 3B). Moreover, the induction of expression of 2 fetal genes, *NPPA* and *NPPB,* after overexpression of native ACTC1 (ACTC1_WT) was absent in the presence of mutant protein (ACTC1_G247D; Figure IIC in the Data Supplement).

Similarly, as seen in immunohistochemistry of the human samples, NRVCMs overexpressing ACTC1_G247D showed an increased cell death as observed by increased TUNEL (Figure 3C) and propidium iodide (Figure 3D) positive cardiomyocytes, compared with the native ACTC1 or control (LacZ) cells. Increased apoptosis was further evident from increased ratios of (cleaved caspase 3)/(total caspase 3) in cells expressing mutant ACTC1_G247D (Figure 3E and 3F). Interestingly though, ratio of (cleaved caspase 12)/(total caspase 12), which is responsible for ER-stress inducible apoptosis was significantly reduced due to ACTC1_G247D expression (Figure IID and IIE in the Data Supplement). Moreover, MTT assay demonstrated reduced cell viability in presence of mutant ACTC1 in NRVCMs (Figure 3G).

Taken together, NRVCM overexpressing mutant ACTC1 exhibited increased apoptosis via activation of caspase 3, attenuated cell proliferation, and sarcomeric defects indicating that the similar effects observed in human patient biopsies are indeed due to ACTC1_G247D mutation.

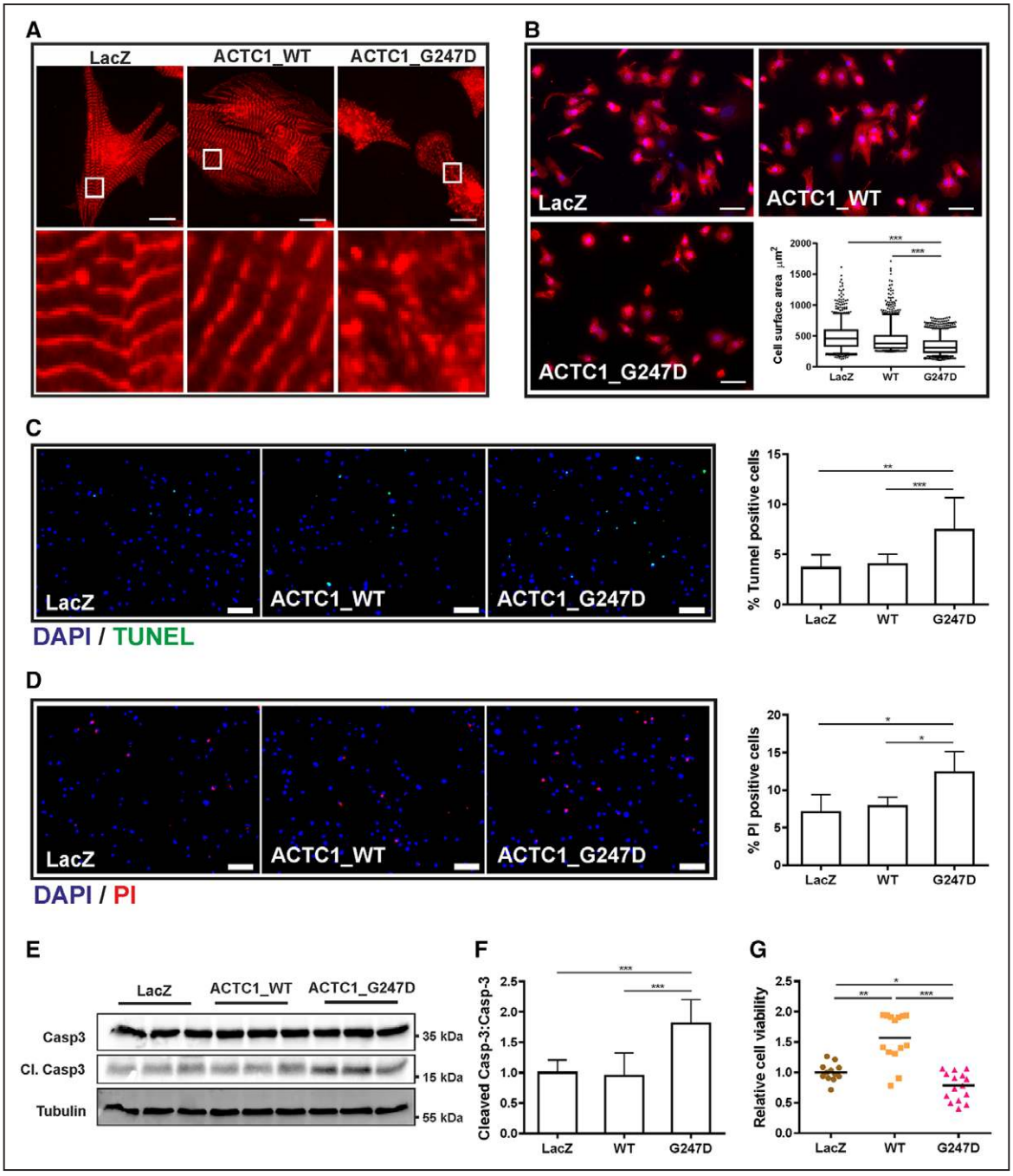

Figure 3. Effects of overexpressed ACTC1 on neonatal rat ventricular cardiomyocytes (NRVCMs).
A, Adenovirus-mediated overexpression of native ACTC1 (ACTC1_WT), mutant ACTC1 (ACTC1_G247D), and control (LacZ). α-actinin antibody-staining (in red). In ACTC1_WT and control (LacZ) overexpressing CM, ordered sarcomere structure, whereas obvious disturbance in presence of overexpressed ACTC1_G247D are observed (scale bar: 50 μm). Respective zoom-in and zoom-out images are shown in **lower** part. **B**, Representative images of cardiomyocytes transfected with LacZ as a control, wild-type or G247D mutant ACTC1, and respective cell surface area shown in a bar graph clearly suggests that G247D mutant reduced cell size in cardiomyocytes. n>1000 cells/group, from 3 independent coverslips. **C**, TUNEL assay for the detection of apoptosis (green); nuclei are counterstained by DAPI (blue) indicates substantial increase in TUNEL positive cells in NRVCM overexpressing mutant ACTC1 compared with the assay in control (LacZ) or in the presence of native ACTC1, but positive TUNEL assay. Adjacent bar graph shows that the TUNEL positive cells were ≈3.6% (LacZ), ≈4.0% (ACTC1_WT), and ≈7.4% (ACTC1_G247D), respectively (P=0.008). **D**, Propidium iodide (PI, red) and nuclear staining (DAPI, blue) of NRVCMs to detect cellular apoptosis and its quantification shown in adjacent bar graph further confirm the increased apoptosis in NRVCMs expressing ACTC1_G247D. **E**, Immunoblot for Caspase 3 (Casp3) and its cleaved product (Cl. Casp3). Tubulin is shown as an endogenous loading control. **F**, Relative densitometry quantification of the ratio of caspase 3/cleaved caspase 3 from (**E**) revealing increased cleaved caspase 3 levels in NRVCMs expressing G247D ACTC1. n=3/group. **G**, Bar graph indicating significantly reduced cell viability in NRVCMs overexpressing the G247D mutant, as determined by MTT assay. n=15/group. Data are presented as the means±SD. Statistical analyses were performed using one-way ANOVA followed by Kruskal-Wallis post hoc test (**B**) or 2-tailed Student t test (**C**–**G**). *P<0.05, **P<0.01, and ***P<0.001. All the experiments are repeated 2 to 3 times. TUNEL indicates terminal deoxynucleotidyl transferase dUTP nick end labeling; and WT, wild-type.

Molecular Dynamics Simulation Studies Reveal Structural and Polymerization Defects in Mutant ACTC1

On the pathogenicity prediction scores of in silico tools, the G247D mutation was designated as highly deleterious and functionally significant. The exchange of the nonpolar, neutral glycine by an acidic polar, negatively charged aspartic acid at residue 247 is likely to affect hydrophobic interactions and folding pattern of the ACTC1 protein. It is well known that during folding of the polypeptide chain, the amino acids with a polar (hydrophilic) side chains are found on the surface of the molecule, while amino acids with nonpolar (hydrophobic) side chains are buried in the interior.

Homology modeling using the SWISS-MODEL workspace[9] and the PyMol tool[10] was performed to determine the structural changes of ACTC1_G247D. Superimposed structures of native and mutant ACTC1 (Figure IIIA in the Data Supplement upper and lower panels) suggest that the drift from hydrophobic to hydrophilic properties are likely to increase the solvent accessible surface area (SASA; calculated SASA for ACTC1_WT is 16484.396 versus 16631.533 for ACTC1_G247D), also predictably affecting the hydrogen bonding and protein folding. Measured distances between the neighboring

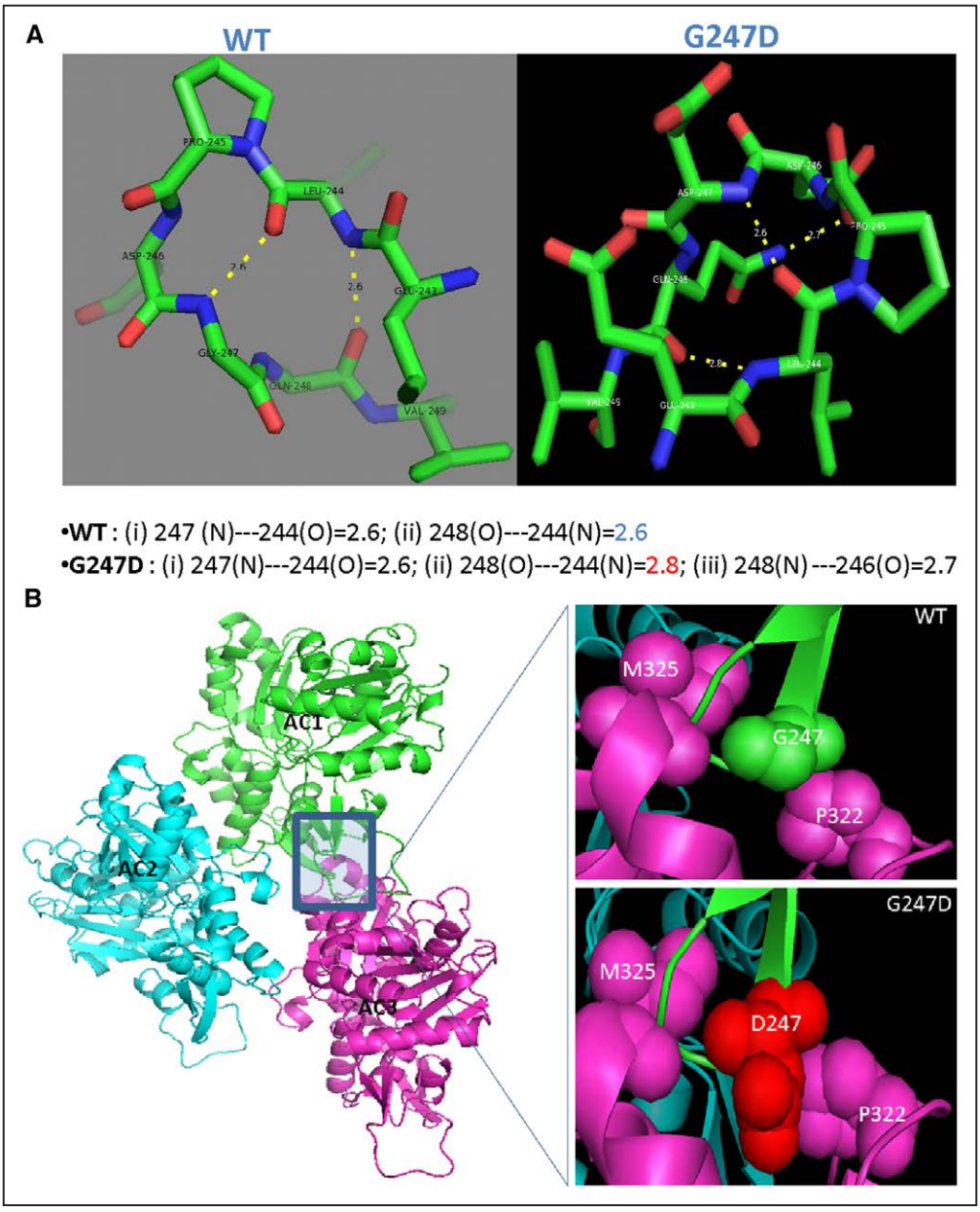

Figure 4. Structural modeling of mutant ACTC1_G247D.
A, Mutant actin (ACTC1_G247D) affects electrostatic interactions in neighboring residues as being marked with yellow, dotted lines, and noted below the image. **B**, Actin trimer (AC1-3) **left**, generated from mutant ACTC1; the area harboring the mutant residue 247 is highlighted (**right**) and clearly shows that the mutant residue lies in close proximity of the point of interaction between adjacent chains. WT indicates wild-type.

residues within the range of 4 Å from the mutational point exactly supported this (native protein, ACTC1_WT: distance between G247>L244 and L244>Q248 were calculated as 2.6 Å; in ACTC1_G247D: L244>Q248 2.8 Å). In addition, Q248 made a new steric contact with D246 (maintained at distance of 2.7 Å; Figure 4A).

Of note, we predicted the polymeric structure of ACTC1 by actin polymerization simulation using a recently proposed Holmes 2010 F-actin model[11] to know whether ACTC1_G247D in silico affects actin polymerization. The mutant residue G247D is located at the interface between 2 monomeric ACTC1 units (chain 1 and 3; Figure 4B), suggesting possible polymerization defects due to the substitution. In contrast, molecular dynamics studies revealed no obvious structural changes between actin-myosin interaction sites as the substitution is distant from the site of interaction (Figure IIIB in the Data Supplement). Further detailed results obtained from molecular dynamics simulations can be read as expanded results in the Data Supplement.

Altogether, molecular dynamics analysis data predicted altered allosteric interactions, reduced protein stability due to increased SASA and due to reduced hydrogen-bond formation efficiency, and subsequently a potential polymerization defect in mutant ACTC1_G247D.

Mutant Human ACTC1_G247D Decreases Myocellular Contractility in Adult Rat Ventricular Cardiomyocytes

Due to the illustrated defects in actin polymerization in human tissue samples and in myocellular expression models (Figures 2 and 3, respectively), we determined the effect of mutant actin on contractility of adult rat ventricular cardiomyocytes overexpressing either native or mutant actin. Treated adult rat ventricular cardiomyocytes were put on glass coverslips to measure cell shortening in response to electrical stimulation of 2.0 Hz. The cell shortening was ≈20% lower in cardiomyocytes infected with mutant ACTC1_G247D (Table IV in the Data Supplement). In addition, other parameters of contraction or relaxation were impaired in NRVCM overexpressing mutant ACTC1_G247D, for example, an increased time-to-peak contraction or reduced rate of contraction, or, a reduced rate of relaxation and prolonged time to peak relaxation (Figure 5A; Table IV in the Data Supplement).

Finally, we investigated the dynamic behavior of mutant ACTC1 in comparison with native protein using fluorescence recovery after photobleaching. Respective GFP-tagged proteins were expressed in NRVCMs using adenoviral transduction. Immunofluorescence microscopy data indicated no severe difference in the localization of either of the overexpressed proteins. However, diffused sarcomeres were still visible with G247D mutant (Figure 5B). Fluorescence recovery after photobleaching analysis revealed dramatic reduction in the recovery of G247D mutant ACTC1 protein after photobleaching compared with the wild-type counterpart (Figure 5C). Over 50% of the wild-type protein was recovered in 40 to 45 minutes; however, even after 80 minutes of measurements, <40% of the G247D mutant protein was recovered (Figure 5C).

Taken together, these results were suggestive of strong actin turnover defects, severely dysfunctional cell contractility in adult rat ventricular cardiomyocytes overexpressing mutant α-actin, and thereby, an impairment of essential myocellular function.

DISCUSSION

Familial (nonsporadic) forms of CHDs are rare but are more likely to be of genetic origin. However, even in familial forms of CHDs a genetic cause may remain elusive in 50% to 70% cases after whole-genome sequencing.[12] This is evidently related to (1) incomplete disease understanding and phenocopies, (2) small CHD families are insufficient for phenotype cosegregation studies of the multiple variants obtained after parallel gene analyses, and (3) from the lack of comprehensive functional analyses of mutant gene variants. ASDs are the third most common type of CHD (estimated incidence: 100 per 100 000 live births) and occur mostly sporadic; it accounts for 7% to 10% of CHD in children but for 25% to 30% of CHD in adult populations.[1] Familial ASD cases are mainly related to mutations in cardiac transcription factors, for example, *NKX2-5*, *GATA4*, and *TBX5*. In a recent case-control study, the ASD phenotype was linked to a marker region on chromosome 4p16 that apparently significantly (9%) contribute to the population-attributable risk of ASD.[13] Here, we describe one of the largest families described so far with autosomal dominant ASD and identified a nonsynonymous mutation in the *ACTC1* gene (encoding the cardiac α-actin). Using a comprehensive investigation including a human cardiac sample, cellular, molecular, and insilico analyses of mutant ACTC1, we demonstrated that this novel mutation led to severe sarcomeric disarray and impaired myocellular contractility due to increased apoptosis and significant alterations in SRF signaling. As a unique feature, *ACTC1* mutation carriers also developed significant and terminal heart failure in the fifth decade indicating an important role of the cardiac α-actin in both, development of the atrial septum and left ventricular function.

Phenotypic Manifestations of Cardiac α-Actin (*ACTC1*) Gene Mutations

So far, inherited forms of ASD mainly resulted from loss-of-function mutations of cardiac transcription fac-

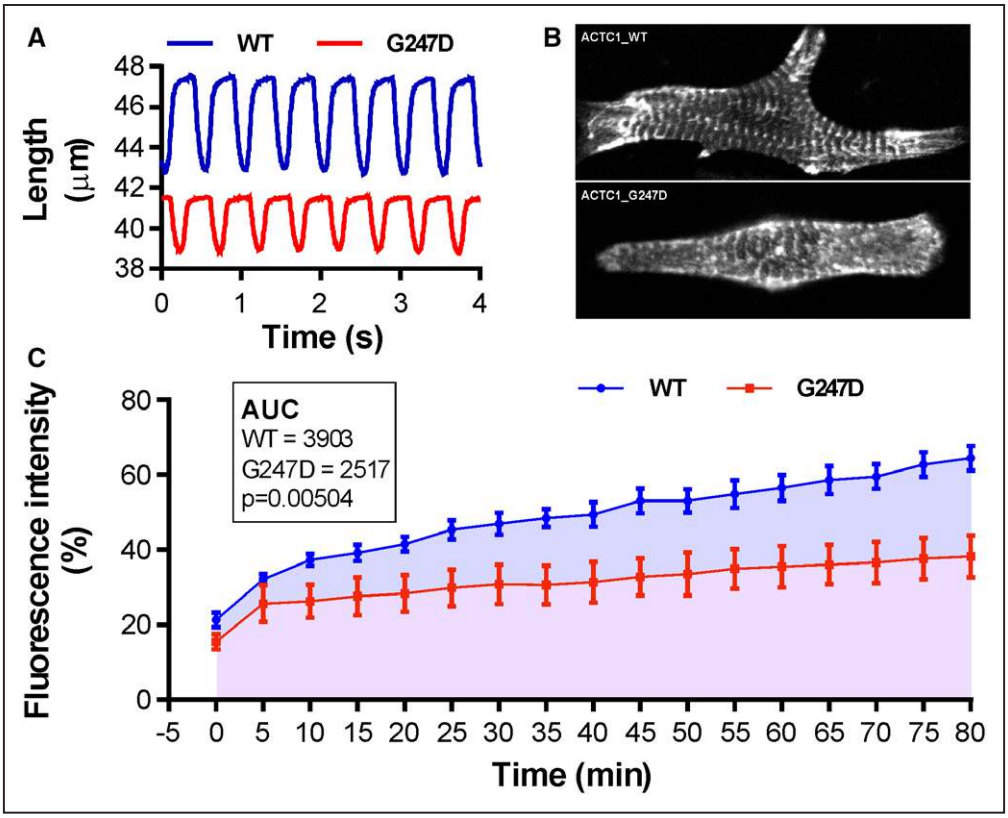

Figure 5. Mechanical properties of native (ACTC1_WT) or mutant (ACTC1_G247D) human a-actin overexpressed in adult rat ventricular CMs. **A**, Representative recording of cell shortening in response to electrical stimulation of 2.0 Hz in adult rat ventricular cardiomyocytes (ARVCMs) infected with adenoviruses overexpressing either native or mutant ACTC1. The cell shortening was ≈20% lower in ARVCMs containing mutant ACTC1_G247D than in ACTC1_WT. **B**, Representative immunofluorescence micrograph showing the sarcomeric localization of the overexpressed GFP (green fluorescent protein)-tagged wild-type and G247D mutant ACTC1 proteins. **C**, Bar graph showing the time-dependent recovery of GFP-tagged native and G247D mutant ACTC1 proteins after photobleaching. Data clearly indicates that the recovery of the mutant protein is severely hampered compared with the wild-type protein. Data are presented as the means±SEM. Area under curve (AUC) was measured using GraphPad Prism 6. Respective AUC (and *P* value) are embedded in the graph. All the experiments are repeated 2 to 3 times. WT indicates wild-type.

tors, in particular, GATA4, GATA6, NKX2-5, and TBX5 that interact in a coordinated fashion for a normal atrial morphogenesis in vivo. Therefore, downstream targets of these transcription factors such as cardiac α-actin, *MYH6* (myosin heavy chain gene 6) are key targets for ASD pathogenesis.[14–17] Five mutations in *ACTC1* (3 nonsynonymous, 1 truncating mutation, and 1 miRNA binding site variant at the 3′-untranslated region region) have thus far been described in patients with isolated ASD-II (Table I in the Data Supplement). Heterozygous mutations in *ACTC1* are associated with isolated ASD are mainly located in the protein's subdomain 1 and adjacent areas (Table I in the Data Supplement). Dysfunction or ablation of cardiac actin causes developmental, cell growth, and polymerization defects, induced apoptosis (at the atrial and ventricular level) leading to a disrupted cardiac differentiation.[18,19]

Of note, mutations in *GATA4*, *TBX5*, and *MYH6* have also been identified in a small fraction of patients with different, but isolated forms of cardiomyopathies (eg, DCM and HCM). Along these lines, the mutant cardiac α-actin (p. G247D) from present study has been identified in one of the largest families with ASD demonstrated clinically later, but severe heart failure as part of the phenotype and further underlined the relevant (left) ventricular function of α-actin. In rat cardiomyocytes, the contractile dysfunction resembling the cellular heart failure phenotype became evident by several experimental lines. To our knowledge, this is the first *ACTC1* mutation with this combined and important phenotype that has been comprehensively characterized. Interestingly, a loss-of-function in the transcription factor *TBX20* mutation has been reported in a comparable disease manifestation (DCM and CHD/ASD) with similar implications for personalized treatment and patient follow-up[20].

Sarcomeric Disarray and Increased Apoptotic Cell Death Caused by the G247D *ACTC1* Mutation

Both, biopsies from human patients and NRVCMs overexpressing the G247D mutation revealed significant sarcomeric disarray. It has been earlier shown that excessive apoptosis plays an important role in the formation of secundum-type ASDs.[3] Here, we show that the

overexpression of G247D mutant ACTC1 significantly enhanced apoptotic cardiomyocyte cell death. Analyses in cardiac biopsies from disease- and mutation carrying patients further confirmed the accelerated apoptosis in human due to G247D mutation. It is unclear whether apoptosis in the carrier of the mutation is triggered directly by the mutation, or whether the present DCM is a secondary effect, as apoptosis has been noted in most DCM cases (about 87%).[21] It becomes clear, however, that the disarray of the Z-bands is not a secondary effect of the DCM since this only occurs in the *ACTC1* mutation carriers. Also in line with these results, relevant cardiomyocyte apoptosis and disorganized sarcomeres have been described for ACTC1-deficient mice.[19] The finding that the ER stress-responsive Caspase 12 was not activated by the G247D mutation is consistent with the results that we could not observe any mutation-associated protein aggregates.

Structural and Polymerization Defects Explain the Phenotype

It is well established to analyze the potential 3D changes in the protein by disease-causing gene mutations. Using a comprehensive approach of the combination of 4 in silico tools, we show that the changes in protein polarity caused by the mutation very likely lead to dramatic changes in protein conformation, and actin polymerization, since the mutation is directly located in the interaction site of 2 monomers (chain 1 and chain 3). Polymerization defects could be confirmed in vitro in NRVCMs, where, filamentous G247D mutant actin was significantly reduced, its rate of polymerization was also strikingly reduced. These findings are further supported by the severe sarcomeric defects, which could be detected in G247D mutation expressing NRVCM and in heart biopsy from patient carrying G247D mutation compared with the respective controls.

Decreased Contractility and Protein Turnover as a Hallmark of the G247D ACTC1 Gene Mutation

Although, we could not detect alteration in actin/myosin interaction by the G247D mutation by in silico analyses, contractility of cardiomyocytes was significantly impaired. Given the polymerization defects described before, it is conceivable that these deficits influence contractility. In cardiomyocytes, actin together with myosin filaments and a large number of scaffolding proteins are organized in a regular contractile units or sarcomeres. It is well established that contracting cardiomyocytes undergo significant actin dynamics, not only involving contractility-dependent exchange of whole filaments but also turnover of actin monomers at the ends of actin filament to ensure appropriate sarcomere length.[22,23] Fluorescence recovery after photobleaching analysis, however, revealed strong actin turnover defects due to incorporation of G247D mutation in cardiac α-actin, which we believe further contributes to the contractility defects. Genetic models of perturbed actin polymerization, such as Lmod2-deficient mouse (Lmod2 promotes actin assembly), have demonstrated that compromised actin polymerization can lead to reduced contractility and left ventricular dilatation, the 2 central hallmarks of DCM.[24] In turn, haploinsufficiency of the actin-depolymerizing factor cofilin-2 was also associated with the development of DCM in mice.[25] Thus, well-orchestrated actin filament assembly is crucial for the maintenance of cardiac contractility and left ventricular dimensions. Taken together, the G247D mutation could account for the late-onset DCM encountered in the affected patients mediated through defective actin filament polymerization.

CONCLUSIONS

A novel nonsynonymous *ACTC1* mutation (p. G247D) was associated with a combined, unique phenotype of ASD-II and DCM with severe heart failure. Immunohistology from an explanted mutation carrier's heart and molecular studies revealed sarcomeric disarray, and increased apoptosis as underlying molecular mechanisms most likely due to actin polymerization and turnover defects. Thus, this study adds comprehensive mechanistic data to the pathogenesis of a cardiac α-actin mutation associated with a complex, combined phenotype. From a translational perspective, our findings emphasize the need for personalized monitoring for the development of late-onset heart failure in patients with ASD (independent of ASD closure). In addition, it is tempting to speculate, whether late-onset DCM might contribute to the development of heart failure after late ASD closure.[26]

ARTICLE INFORMATION

Received February 18, 2019; accepted July 19, 2019.

The Data Supplement is available at https://www.ahajournals.org/doi/suppl/10.1161/CIRCGEN.119.002491.

Correspondence

Derk Frank, MD, Universitatsklinikum Schleswig-Holstein, Arnold-Heller-Str 3, Haus 6 Kiel, D-24105, Germany. Email derk.frank@uksh.de

Affiliations

Department of Internal Medicine III, Cardiology and Angiology, University Medical Center Schleswig-Holstein, Campus Kiel (D.F., A.Y.R., A. Bernt, A. Borlepawar, P.U., N.F.). Institute for Genetics of Heart Diseases (IfGH), Department of Cardiovascular Medicine (C.F., S.D., B.S., Ellen Schulze-Bahr, S.P., G.S., A.U., Eric Schulze-Bahr), Institute of Physiology II (W.A.L.), and Institute for Human Genetics (C.F), University Hospital Münster. Division of Molecular Genetic Epidemiology, German Cancer Research Center (DKFZ), Heidelberg (P.Y.). Institute of Pharmacology and Toxicology, University

Medical Center Göttingen (W.H.-Z.). Institute of Pathology, University of Duisburg-Essen (H.A.B.). Center for Molecular Medicine Cologne (CMMC), Proteomics Facility, University of Cologne (M.K.). Co-affiliated with DZHK (German Centre for Cardiovascular Research), sites Hamburg/Kiel/Lübeck and Göttingen, Germany (D.F., A.Y.R., A. Bernt, A. Borlepawar, W.H.-Z., W.A.L., N.F.).

Acknowledgments

We thank all patients participating in the study and to physicians of the heart failure unit (Jörg Stypmann and Markus Engelen) of the Department of Cardiovascular Medicine, University Hospital Münster, and Kurt Minderjahn (Emden). Elvira Deravanessian supported technical assistance in genotyping, Martina Raetz in pedigree drawing. Eva Wardelmann (Institute for Pathology at the University Hospital Münster) kindly provided pathology slices of the heart. Matthias Seidl (Institute of Pharmacology and Toxicology, University of Münster) took fluorescent tissue images of a cardiac sample. Dr Schulze-Bahr was supported by the Interdisciplinary Center for Clinical Research of the University of Münster (grant: Schu1/031/07).

Sources of Funding

Dr Frank was supported by the Christian-Albrechts-University Kiel as well as the eMed program (SYMBOL HF consortium) of the BMBF. Drs Frank, Frey, Zimmermann, and Schulze-Bahr also received funding from the DZHK (German Center for Cardiovascular Research).

Disclosures

None.

REFERENCES

1. Geva T, et al. Atrial septal defects. *Lancet.* 2014;383:1921–1932. doi: 10.1016/S0140-6736(13)62145-5
2. Sun YP, et al. Patent foramen ovale and stroke. *Circ J.* 2016;80:1665–1673. doi: 10.1253/circj.CJ-16-0534
3. Nadeau M, et al. An endocardial pathway involving Tbx5, Gata4, and Nos3 required for atrial septum formation. *Proc Natl Acad Sci USA.* 2010;107:19356–19361. doi: 10.1073/pnas.0914888107
4. Kirk EP, et al. Mutations in cardiac T-box factor gene TBX20 are associated with diverse cardiac pathologies, including defects of septation and valvulogenesis and cardiomyopathy. *Am J Hum Genet.* 2007;81:280–291. doi: 10.1086/519530
5. McBride KL, et al. NOTCH1 mutations in individuals with left ventricular outflow tract malformations reduce ligand-induced signaling. *Hum Mol Genet.* 2008;17:2886–2893. doi: 10.1093/hmg/ddn187
6. Matsson H, et al. Alpha-cardiac actin mutations produce atrial septal defects. *Hum Mol Genet.* 2008;17:256–265. doi: 10.1093/hmg/ddm302
7. Kumar A, et al. Rescue of cardiac alpha-actin-deficient mice by enteric smooth muscle gamma-actin. *Proc Natl Acad Sci USA.* 1997;94:4406–4411. doi: 10.1073/pnas.94.9.4406
8. Olson TM, et al. Actin mutations in dilated cardiomyopathy, a heritable form of heart failure. *Science.* 1998;280:750–752. doi: 10.1126/science.280.5364.750
9. Guex N, et al. SWISS-MODEL and the Swiss-PdbViewer: an environment for comparative protein modeling. *Electrophoresis.* 1997;18:2714–2723. doi: 10.1002/elps.1150181505
10. DeLano WL. Use of PYMOL as a communications tool for molecular science. *Abstr Pap Am Chem S.* 2004;228:U313.s–U314.s
11. Splettstoesser T, et al. Structural modeling and molecular dynamics simulation of the actin filament. *Proteins.* 2011;79:2033–2043. doi: 10.1002/prot.23017
12. Blue GM, et al. Advances in the genetics of congenital heart disease: a clinician's guide. *J Am Coll Cardiol.* 2017;69:859–870. doi: 10.1016/j.jacc.2016.11.060
13. Cordell HJ, et al. Alpha-cardiac myosin heavy chain (MYH6) mutations affecting myofibril formation are associated with congenital heart defects. *Hum Mol Genet.* 2010;19:4007–4016.
14. Granados-Riveron JT, Ghosh TK, Pope M, Bu'Lock F, Thornborough C, Eason J, Kirk EP, Fatkin D, Feneley MP, Harvey RP, Armour JA and David Brook J. Alpha-cardiac myosin heavy chain (MYH6) mutations affecting myofibril formation are associated with congenital heart defects. *Human molecular genetics.* 2010;19:4007-16.
15. Posch MG, et al. Cardiac alpha-myosin (MYH6) is the predominant sarcomeric disease gene for familial atrial septal defects. *PLoS One.* 2011;6:e28872. doi: 10.1371/journal.pone.0028872
16. Ching YH, et al. Mutation in myosin heavy chain 6 causes atrial septal defect. *Nat Genet.* 2005;37:423–428. doi: 10.1038/ng1526
17. Maitra M, et al. Interaction of gata4 and gata6 with Tbx5 is critical for normal cardiac development. *Dev Biol.* 2009;326:368–377. doi: 10.1016/j.ydbio.2008.11.004
18. Lamers WH, et al. Cardiac septation: a late contribution of the embryonic primary myocardium to heart morphogenesis. *Circ Res.* 2002;91:93–103. doi: 10.1161/01.res.0000027135.63141.89
19. Abdelwahid E, et al. Cellular disorganization and extensive apoptosis in the developing heart of mice that lack cardiac muscle alpha-actin: apparent cause of perinatal death. *Pediatr Res.* 2004;55:197–204. doi: 10.1203/01.PDR.0000100900.56627.E1
20. Zhou YM, et al. A novel TBX20 loss-of-function mutation contributes to adult-onset dilated cardiomyopathy or congenital atrial septal defect. *Mol Med Rep.* 2016;14:3307–3314. doi: 10.3892/mmr.2016.5609
21. Glumac S, et al. Apoptosis in endomyocardial biopsies from patients with dilated cardiomyopathy. *Folia Biol (Praha).* 2016;62:207–211.
22. Littlefield R, et al. Actin dynamics at pointed ends regulates thin filament length in striated muscle. *Nat Cell Biol.* 2001;3:544–551. doi: 10.1038/35078517
23. Skwarek-Maruszewska A, et al. Contractility-dependent actin dynamics in cardiomyocyte sarcomeres. *J Cell Sci.* 2009;122(pt 12):2119–2126. doi: 10.1242/jcs.046805
24. Pappas CT, et al. Knockout of Lmod2 results in shorter thin filaments followed by dilated cardiomyopathy and juvenile lethality. *Proc Natl Acad Sci USA.* 2015;112:13573–13578. doi: 10.1073/pnas.1508273112
25. Subramanian K, et al. Cofilin-2 phosphorylation and sequestration in myocardial aggregates: novel pathogenetic mechanisms for idiopathic dilated cardiomyopathy. *J Am Coll Cardiol.* 2015;65:1199–1214. doi: 10.1016/j.jacc.2015.01.031
26. Schubert S, et al. Left ventricular conditioning in the elderly patient to prevent congestive heart failure after transcatheter closure of atrial septal defect. *Catheter Cardiovasc Interv.* 2005;64:333–337. doi: 10.1002/ccd.20292